

Article

Not peer-reviewed version

# New Insight into Geochemistry and Mineralogy of Deep Caves in Croatian Karst and Its Implications for Paleoenvironmental Reconstructions

[Dalibor Paar](#) , [Stanislav Frančišković-Bilinski](#) <sup>\*</sup> , [Nenad Buzjak](#) , Krešimir Maldini

Posted Date: 24 February 2025

doi: 10.20944/preprints202502.1805.v1

Keywords: Dinaric karst; deep caves; geochemistry; mineralogy; magnetic susceptibility



Preprints.org is a free multidisciplinary platform providing preprint service that is dedicated to making early versions of research outputs permanently available and citable. Preprints posted at Preprints.org appear in Web of Science, Crossref, Google Scholar, Scilit, Europe PMC.

Copyright: This open access article is published under a Creative Commons CC BY 4.0 license, which permit the free download, distribution, and reuse, provided that the author and preprint are cited in any reuse.

*Article*

# New Insight into Geochemistry and Mineralogy of Deep Caves in Croatian Karst and Its Implications for Paleoenvironmental Reconstructions

Dalibor Paar <sup>1</sup>, Stanislav Frančišković-Bilinski <sup>2,\*</sup>, Nenad Buzjak <sup>3</sup> and Krešimir Maldini <sup>4</sup>

<sup>1</sup> Department of Physics, Faculty of Science, University of Zagreb, Bijenička c. 32, 10000, Zagreb, Croatia; dpaar@phy.hr

<sup>2</sup> Ruđer Bošković Institute, Bijenička c. 54, 10002, Zagreb, Croatia; francis@irb.hr

<sup>3</sup> Department of Geography, Faculty of Science, University of Zagreb, Trg Marka Marulića 19, 10000 Zagreb, Croatia; nbuzjak@geog.pmf.hr

<sup>4</sup> Department of Monitoring, Main Water Laboratory (MWL), Josip Juraj Strossmayer Water Institute, Ulica Grada Vukovara 220, 10000 Zagreb, Croatia; kmaldini@institutjjs.hr

\* Correspondence: francis@irb.hr

**Abstract:** This study examines speleothems, sediments, rock, and water to assess geochemical and mineralogical processes in deep karst systems. Focusing on Slovačka jama cave (-1,320 m deep) and the Velebita cave system (-1,026 m deep), we identify elemental and mineralogical anomalies that provide valuable records of element transport, mineral formation, and paleoenvironmental changes. Heavy metal anomalies at 300–400 m of depth in Slovačka jama indicate a complex interplay of geological conditions, geomorphological processes, atmospheric deposition, and potential anthropogenic influences. Factor analysis reveals two elemental associations: (1) Fe, Pb, Cu, and Zn, linked to terrigenous aluminosilicates, and (2) Cd, Cr, Mo, and Ni, suggesting airborne or geological sources. Mineralogical analysis confirms the dominance of calcite, with quartz, clay minerals, feldspars, magnetite, and goethite also detected. High magnetic susceptibility values in sediment-rich samples suggest Fe-rich mineral inputs from weathering, biogenic activity, or industrial sources. Ba anomalies in feldspar-rich samples and Sr accumulation at depth indicate distinct geochemical processes. These findings enhance our understanding of deep karst geochemistry, crucial for paleoenvironmental reconstructions and groundwater protection.

**Keywords:** Dinaric karst; deep caves; geochemistry; mineralogy; magnetic susceptibility

## 1. Introduction

The Croatian karst is primarily situated in the Dinaric karst, globally recognized as the locus typicus of Classical Karst, with a smaller portion extending into isolated karst areas of the Pannonian Basin [1]. Karst landscapes are among the most complex and hydrologically dynamic environments on Earth, characterized by high permeability, rapid water flow, and intricate interactions between surface and underground processes [2,3]. Despite its significance, the geochemistry and mineralogy of Croatian caves remained largely unexplored until recent years.

To address this research gap, a study was launched in 2016 with the aim of identifying speleothem proxies suitable for paleoenvironmental reconstructions [4]. The primary focus was to analyze the elemental composition and mineralogy of speleothems from various Croatian karst sites and assess how distinct climatic, geological, geomorphological and hydrological conditions influence their characteristics. A total of 37 speleothem samples from 32 caves across different geomorphological and climatic zones were analyzed. The elemental composition of 30 elements was determined using ICP-MS, while mineral phases—including calcite, quartz, dolomite, muscovite/illite, chlorite, and plagioclase—were identified via XRD. Among the most abundant

elements, in addition to calcium, those exceeding 500 mg/kg included Al, Fe, Si, and Mg. Statistical analysis using boxplot methods revealed significant anomalies in the deep caves of Northern Velebit, particularly in Lukina jama, where extreme values were recorded for Pb, Cu, Zn, Mn, Ni, Cr, Co, Ba, K, Mg, Li, Be, Al, U, Si, Ti, W, Fe, and As. These findings align with previous studies indicating that deep karst environments often record significant geochemical anomalies due to their complex hydrological and tectonic histories [4,5].

Given that the most pronounced anomalies were identified in the deep caves of Velebit Mountain, a new study was initiated to investigate geochemical and mineralogical variations at depths of up to 1,320 m in Slovačka jama cave and 1,026 m in the Velebita cave system. These caves are located within a geologically complex karst terrain shaped by intensive tectonics, particularly during the Neotectonic period, which, in conjunction with prolonged karstification, has resulted in intricate subsurface structures (Figure 1). Recent research suggests that such deep cave environments provide valuable records of past climatic and geochemical conditions, making them critical sites for paleoenvironmental studies [6,7].

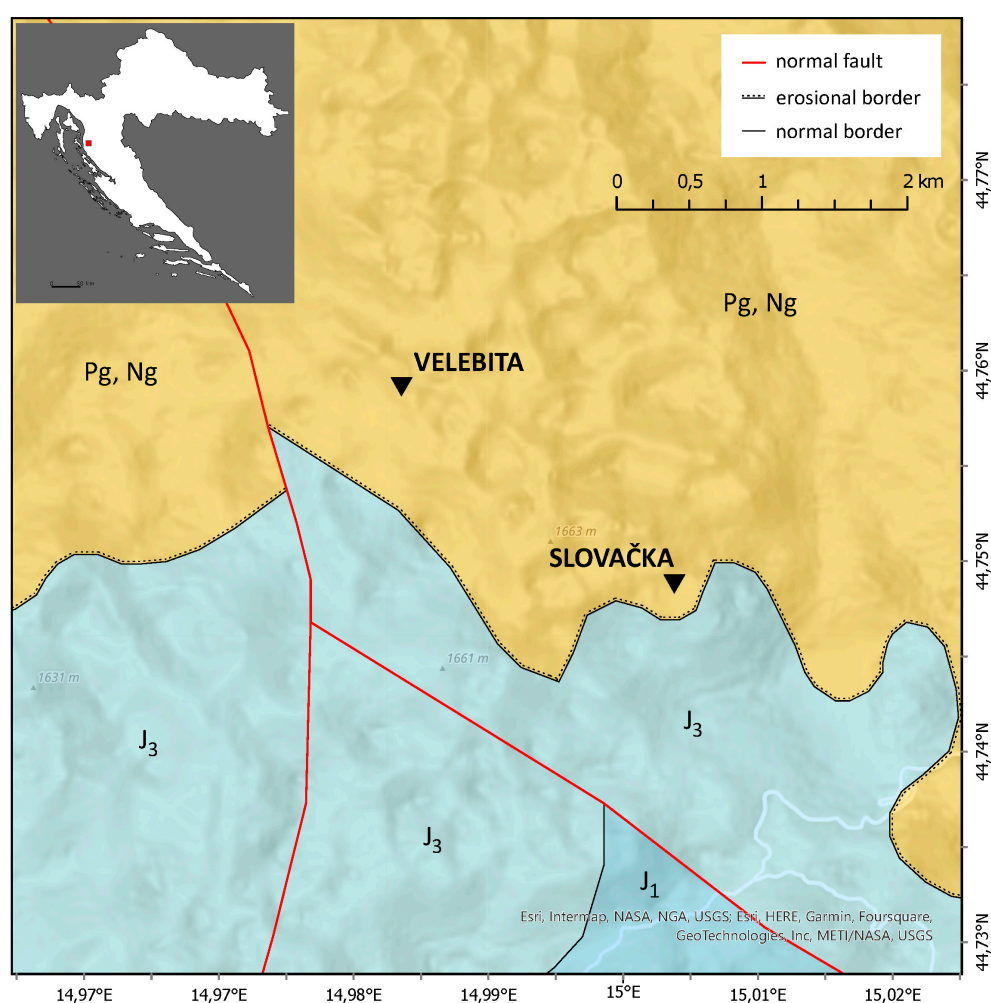


**Figure 1.** Position of Velebita cave system and Slovačka jama cave on the geological map of Velebit Mt. Litostratigraphical legend: J1 – limestones and dolomites (Lower Jurassic), J3 - limestones and dolomites (Upper Jurassic), Pg, Ng – carbonate breccia (Peleogene, Neogene). Map: Croatian Geological Survey (2009): Geological map of the Republic of Croatia M 1:300,000, Zagreb.

The study of karst systems is not only important for understanding past environmental changes but also has direct implications for water resource management. Karst aquifers are highly vulnerable to contamination due to their rapid recharge and direct connectivity between surface and groundwater systems [8]. It is estimated that approximately 25% of the world's population relies on groundwater extracted from karst aquifers [9]. Understanding the hydrogeochemical dynamics of

these systems is particularly challenging due to their extreme heterogeneity [10,11]. Investigations in deep caves offer a unique opportunity for in situ sampling, measuring and analyses of karst processes in deep karst (>1.000 m), shedding light on the mechanisms controlling element mobility, mineral formation, and potential anthropogenic impacts [12] influencing epiphreatic and phreatic zone important for regional aquifer characteristics.

In our study, we expand upon previous research by analyzing multiple sampling media—including speleothems, cave clastic sediments, and water chemistry—to assess their geochemical and mineralogical properties and identify potential interactions. Such multi-proxy approaches remain relatively rare in karst research, particularly concerning cave sediments and water chemistry. However, several relevant studies provide useful comparisons. For instance, Rozkowski et al. [13] examined the migration and concentration of heavy metals in infiltration waters within a carbonate massif, linking these variations to both natural mobility and anthropogenic influences. Similarly, Pons-Branchu et al. [14] utilized urban speleothems to reconstruct heavy metal pollution histories in shallow groundwater systems, demonstrating how speleothem chemistry can serve as a long-term record of environmental changes. Other studies have explored the role of cave sediments and particulate matter in element transport, with Allan et al. [15] analyzing lead concentrations and isotopic compositions in Belgian caves to distinguish between anthropogenic and natural sources. More recently, Xu and Zeng [16,17] investigated heavy metal contamination in cave water and suspended particulate matter, respectively, underscoring the importance of geochemical monitoring in karst systems.

The primary aim of this study is to systematically investigate geochemical and mineralogical variations in deep karst cave environments, assess the potential interactions between different sampling media, and evaluate their implications for paleoenvironmental reconstructions and pollution monitoring.

## 2. Materials and Methods

### 2.1. Sample Preparation and Analysis

Speleothems for this study were collected with minimal disturbance to the cave environment, ensuring that natural formations remained intact. The sampling locations in the Velebita cave system and Slovačka jama cave are shown in Figure 2. Samples were collected from sites where carbonate precipitation and karst drainage networks facilitate speleothem growth [18–21]. These locations were carefully selected to ensure representative data on geochemical and mineralogical processes within the deep karst environment.

Samples were carefully handled to prevent contamination, washed with distilled water, air-dried, and then homogenized using a Retsch RM 200 mortar grinder. Whole speleothems were crushed to obtain representative powders incorporating all growth layers. From these, 1 g of material was used for ICP-MS and XRD analysis.

For elemental analysis, 0.1 g of powdered sample was digested in a mixture of suprapur nitric and puriss hydrochloric acid, heated in an Anton Paar Multiwave 3000 Oven following ISO 11466 standards. ICP-MS (Elan 9000, Perkin Elmer) was used to determine elemental concentrations, employing internal standards (Ge, Rh, In, Re) according to ISO 17294-1 and ISO 17294-2. Precision (RSD) was within 10%, and accuracy was verified using reference material (RTC CNS392-050), with results aligning within 15% of certified values. Only two samples (ZSDV-64, ZSDV-70) had values below the quantification limit for Tl (5.4%).

Mineralogical composition was identified using X-ray diffraction (XRD) with a Philips X-Pert MPD diffractometer, analyzed via Powder Diffraction File (1997) and X'Pert HighScore software. Semi-quantitative mineralogy followed [22].

Magnetic susceptibility (MS) was measured using an SM30 (ZH Instruments) susceptibility meter, capable of detecting low-magnetic and diamagnetic materials such as limestone and quartz. Measurements were performed three times per sample, with the mean value recorded to ensure accuracy.



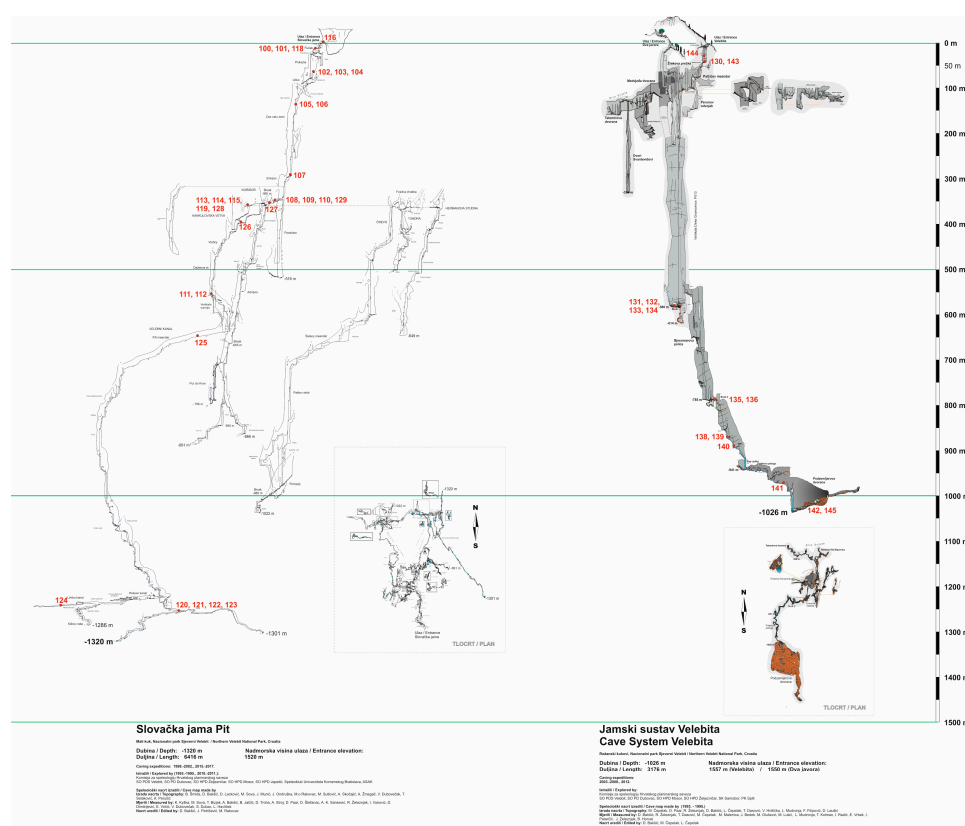


**Figure 2.** Sampling locations in Slovačka jama and Velebita cave system, Velebit Mt., Croatia. Map: Speleological Committee of CMA (1993-2017).

## 2.2. Statistical Analysis

Statistical analyses were conducted using Statistica 6.0 [23] and included:

- Descriptive Statistics:** Basic parameters (mean, median, standard deviation, skewness, kurtosis) were calculated to summarize the dataset. Pearson's correlation coefficients were determined to assess relationships between elements ( $p < 0.05$ ).
- Boxplot Analysis:** Used to identify anomalies in sediment samples based on interquartile range, with outliers and extreme values defined according to Tukey [24] and Reimann et al. [25].
- Cluster Analysis (Q-mode):** Performed to group similar samples using a hierarchical method, distinguishing sample clusters rather than elemental correlations [26].
- Factor Analysis:** Applied to reduce variable complexity and identify key natural or anthropogenic influences, assuming correlations between multiple elements are driven by a smaller set of main factors [27,28].

## 3. Results and Discussion

### 3.1. Mineralogical Analysis Using X-Ray Diffraction

Mineralogical analysis using X-ray diffraction (XRD) identified 10 minerals across the samples: carbonates (calcite, dolomite), silicates (quartz, clay minerals—kaolinite, muscovite, chlorite, montmorillonite, and feldspar—plagioclase), spinels (magnetite), and oxihydroxides (goethite). This method is qualitative, with a detection limit of ~5%.

As expected, calcite was present in all samples due to the karstic environment, where speleothems form by limestone dissolution and carbonate precipitation (Table A1). Dolomite appeared in only three rock samples from Slovačka jama (ZSDV-118, ZSDV-122, ZSDV-123), suggesting localized geochemical variations. In eight samples, only calcite was detected (e.g., ZSDV-101, ZSDV-111, ZSDV-113).

Quartz, the second most abundant mineral, was found in 36 of 45 samples, likely originating from fine-grained clastic sediments introduced into the cave system [4]. Similar findings were reported in karstic river sediments [29].

Among clay minerals, muscovite and chlorite were most common, followed by kaolinite and montmorillonite. Samples containing at least two clay minerals (e.g., ZSDV-105, ZSDV-107, ZSDV-110) often coincided with geochemical anomalies and high magnetic susceptibility (MS). Notably, ZSDV-105 and ZSDV-107, from the same vertical channel of Slovačka jama, displayed strong similarities despite a 145 m elevation difference.

Feldspars (plagioclase) were detected in only four samples (ZSDV-112, ZSDV-126, ZSDV-130, ZSDV-133), all from channel-bottom sediments in Slovačka jama and Velebita cave system. Among Fe-bearing minerals, magnetite and goethite were identified in samples from Slovačka jama, with ZSDV-110 being the only one containing both. These minerals may indicate past hydrothermal influences or iron mobilization within the cave system.

The relationships between mineralogical composition, ICP-MS element concentrations, and magnetic susceptibility will be further explored in the discussion.

### 3.2. ICP-MS Analysis, Magnetic Susceptibility, and Elemental Anomalies

ICP-MS analysis results for speleothems and water samples are presented in Table A2 and Table A3. While elemental concentrations in speleothems will be statistically analyzed in later sections, water sample data were not statistically evaluated due to the limited number of results ( $n = 3$ ).

Magnetic susceptibility (MS) values, expressed in  $10^{-3}$  SI units, range from 0.000 to 0.168, with the highest value recorded in ZSDV-107 (Table A9). MS variations will be discussed in relation to elemental composition in later sections.

Elemental anomalies identified using the boxplot statistical method (Table A4) indicate that ZSDV-107 has the highest number of anomalies, followed by ZSDV-127. Outliers and extremes were observed for multiple elements, suggesting localized geochemical or environmental influences. These patterns will be further explored in the discussion.

### 3.3. Q-Modality Cluster Analysis

Q-mode cluster analysis results are presented in Table A5 and Table A6. Three clusters were identified:

- Cluster 1 (Deepest, avg. depth 664.25 m): Composed of 8 sediments, 4 speleothems, and 4 rock samples, showing a moderate concentration of heavy metals.
- Cluster 2 (Intermediate, avg. depth 440.25 m): Contains 10 rocks, 9 speleothems, and 1 sediment sample, with the lowest heavy metal concentrations.
- Cluster 3 (Shallowest, avg. depth 323.89 m): Includes 8 sediments and 1 rock sample, exhibiting the highest heavy metal concentrations (except for Ni), suggesting accumulation near the surface due to airborne pollution, soil leaching, and surface runoff.

Heavy metals appear to migrate downward, accumulating first in shallow cave sections before being rinsed and redeposited in deeper zones. These transport mechanisms require further investigation.

Strontium concentrations notably increase in the deepest sections, but current data are insufficient to draw firm conclusions, warranting further research. Additionally, calcium concentrations in speleothems are lowest in shallow sections, nearly four times lower than in the middle depth, where they peak.

### 3.4. Factor Analysis

Factor analysis was performed on 16 variables, including sample depth and elemental concentrations (Al, Be, Ca, Cd, Co, Cr, Cu, Fe, Li, Mn, Ni, Pb, Si, Sr, Zn). The results explained 83.7% of total variability, indicating a strong statistical model. Factor scores (Table A8) indicate the degree

of influence of each factor on individual samples, while factor loadings (Table A7) reveal relationships between variables.

### Interpretation of Factors

Factor 1: Dominated by the aluminosilicate component, indicating high influence from soil and non-carbonate rocks. Ca shows a strong negative correlation, while Fe and Mn likely originate from natural aluminosilicates. Zn, Pb, and Co may have either natural or anthropogenic sources but strongly correlate with this factor.

Factor 2: Primarily associated with Cd, Cr, and Ni, forming a distinct elemental group. Their origin could be either atmospheric deposition from distant pollution sources or natural geological processes, differing from elements in Factor 1.

Factor 3: Shows negative correlations with depth and Sr, consistent with Q-mode cluster analysis, which indicated that Sr concentrations increase with depth.

These factors provide valuable insights into the geochemical processes affecting element distribution in the studied cave system.

### 3.5. Discussion

This section integrates mineralogical, geochemical, and geophysical data to explain the origin of detected elements and minerals, their distribution, and interactions within the cave system.

#### 3.5.1. Mineralogy and Magnetic Susceptibility (MS) Relationships

Samples containing only calcite (or calcite + dolomite) exhibited very low MS values ( $\leq 0.002 \times 10^{-3}$  SI units) and showed few or no elemental anomalies. A notable exception was sample ZSDV-123, where an Mg anomaly coincided with the presence of dolomite, confirming its natural origin. This sample, collected from a horizontal channel at the bottom of Slovačka jama, suggests the presence of dolomitic bedrock at depth, though current geological maps lack subsurface detail.

In contrast, samples containing clay minerals displayed higher MS values and numerous elemental anomalies. The most abundant clay minerals were chlorite and muscovite, with kaolinite and montmorillonite present in smaller amounts. Chlorite, commonly found in metamorphic and volcanic environments, is known to contain Fe and Mn, which may explain the observed high MS values. It is likely formed through low-grade metamorphism or weathering of mafic minerals (e.g., pyroxenes, amphiboles, biotite).

#### 3.5.2. Elements and Magnetic Susceptibility (MS) Relationships

Table A10 presents the correlations between magnetic susceptibility (MS) and chemical elements in the studied samples. MS exhibits strong to excellent correlations with Al, Ba, Be, Bi, Ca, Co, Cu, Fe, Li, Mn, Pb, Rb, Ti, Tl, and Zn, suggesting that MS can serve as a reliable proxy for detecting locations with elevated concentrations of these elements.

#### 3.5.3. Potential Sources of Clay Minerals and Heavy Metals

Clay minerals in the samples studied may originate from multiple sources:

1. Terra rossa contribution: Similar to findings from Istria (Durn et al., 2007), terra rossa in karst regions often forms from insoluble residues of limestone and dolomite, but can also contain aeolian dust, volcanic debris, and transported sedimentary particles. These external sources may have introduced heavy metals over geological timescales.
2. Aeolian and volcanic inputs: Past atmospheric processes could have deposited metal-rich dust and volcanic ash, leading to localized heavy metal anomalies.
3. Hydrothermal activity: Though not confirmed, hydrothermal processes might have contributed to mineral transformations and heavy metal enrichment in deeper cave sediments.

### 3.5.4. Feldspars and Their Geochemical Significance

Feldspars (plagioclase) were detected in only four samples, often alongside clay minerals. While no major anomalies were associated with feldspar-rich samples, Ba anomalies were identified in ZSDV-130 and ZSDV-133. Since alkaline barium feldspars can form through Ba substitution for K in feldspar structures, it is likely that crystallization processes in igneous or metamorphic rocks played a role in Ba enrichment.

### 3.5.5. Iron Minerals and Their Origins

Two Fe-rich minerals were detected:

1. Magnetite (spinel) – Found in cave sediments, possibly originating from:
  - a) Natural sources, such as weathering of bauxites (known to occur in Velebit Mt.).
  - b) Biogenic activity, as some microorganisms can precipitate magnetite.
  - c) Anthropogenic pollution, transported via airborne deposition.
2. Goethite (oxyhydroxides) – Typically forms through lateritic weathering and was found in samples where Fe anomalies were detected.

Samples ZSDV-107 and ZSDV-127, both from Slovačka jama, exhibited Fe anomalies and contained magnetite, suggesting an unusual geochemical environment in these sediments.

### 3.5.6. An Unusual Geochemical Outlier

Sample ZSDV-107 (285 m depth, Slovačka jama) displayed:

- The highest MS value ( $0.168 \times 10^{-3}$  SI units).
- A complex mineralogical composition (calcite, quartz, all four clay minerals, magnetite).
- Multiple elemental anomalies, including extremes for Al, B, Co, Mn, Na, Tl and outliers for Ba, Be, Cr, Cu, Fe, K, Pb, Rb, Ti, U, Zn.

These anomalies suggest a unique depositional or geochemical process, potentially involving multiple metal sources (natural and anthropogenic), deep sediment accumulation, and prolonged geochemical transformations. Further geochemical and isotopic studies are needed to fully understand its formation.

### 3.5.7. Factor Analysis and Elemental Associations

Factor analysis revealed a distinct grouping of Cd, Cr, and Ni, separate from other heavy metals. This suggests:

- Different sources or transport mechanisms compared to Zn, Pb, and Co.
- Possible atmospheric deposition (long-range transport of industrial pollutants).
- Alternatively, a unique natural geological source distinct from the aluminosilicate fraction.

Our results indicate that heavy metal anomalies in cave sediments and speleothems can be attributed to a combination of natural geochemical processes and potential atmospheric deposition. Similar findings were reported by Rozkowski et al. [13], who examined heavy metal transport within the unsaturated and saturated zones of a carbonate massif in Poland. Their study highlighted the influence of infiltration processes on metal migration, which aligns with our observations of metal transport from shallow to deep cave sections in Slovačka jama and the Velebita cave system. The accumulation of elements like Pb, Zn, and Cu in cave sediments suggests both allochthonous input (surface-derived material) and internal redistribution within the karst system.

Moreover, our analysis supports the idea that speleothems can serve as long-term environmental archives, recording changes in metal concentrations over time. Pons-Branchu et al. [30] demonstrated that speleothems in urban settings provide valuable records of historical heavy metal pollution, showing enrichment in Pb, Mn, V, Cu, Cd, and Al due to anthropogenic contamination. While our study is focused on deep karst environments rather than urban speleothems, the detection of Cd, Cr, and Ni as a distinct elemental association (factor analysis) raises the possibility of airborne metal deposition from distant pollution sources, a hypothesis also considered in their research.



The role of lead in karst environments has been extensively studied, with Allan et al. [15] demonstrating how Pb concentrations and isotopic ratios in speleothems can be used to trace atmospheric pollution since the Industrial Revolution. While Pb anomalies in our samples could originate from natural sources (aluminosilicate components), the presence of additional metals associated with industrial activity suggests that long-range atmospheric transport may also contribute. Further isotopic analysis could help differentiate between these sources.

Overall, the combined use of mineralogical, geochemical, and statistical methods provided a comprehensive understanding of element distribution in deep karst environments, highlighting both natural and anthropogenic influences on cave sediments.

#### 4. Conclusions and Future Research

This study highlights the complex geochemical interactions in deep karst environments, with speleothems and sediments serving as important archives of elemental transport and potential pollution pathways. Our results align with findings by Rozkowski et al. [13], Pons-Branchu et al. [30], and Allan et al. [15], all of whom investigated metal migration and accumulation in carbonate environments. The detection of heavy metal anomalies in sediments and speleothems suggests that karst systems are influenced by both natural geochemical processes and possible anthropogenic inputs.

Mineralogical analysis confirmed that calcite is the dominant mineral in all samples, as expected in a karst environment, while quartz was present in most samples, likely introduced via fine-grained clastic sediments. Clay minerals, including muscovite, chlorite, kaolinite, and montmorillonite, were found to be associated with higher magnetic susceptibility (MS) and heavy metal anomalies, indicating their role in metal transport. Feldspars, though rare, were linked to barium anomalies, suggesting the formation of alkaline barium feldspars. The presence of iron minerals such as magnetite and goethite, particularly in cave sediments, points to multiple possible origins, including natural sources such as bauxites, biogenic activity, or even airborne pollution.

Geochemical and statistical analyses provided additional insights into element distribution and transport within the cave system. Samples composed solely of calcite or calcite with dolomite exhibited the lowest MS values, indicating minimal influence from non-carbonate materials, whereas samples containing clay minerals displayed elevated MS values and a high number of elemental anomalies, supporting the hypothesis that clays play a significant role in metal retention. Boxplot analysis identified the highest number of anomalies in samples ZSDV-107 and ZSDV-127, suggesting a complex geochemical environment. Q-mode cluster analysis revealed that heavy metals are more concentrated in shallow cave sections, likely due to airborne deposition or surface leaching, with subsequent transport and accumulation in deeper parts of the cave system. Factor analysis identified cadmium, chromium, and nickel as a distinct group, indicating a different origin from other heavy metals, potentially related to atmospheric deposition or specific geological sources.

While this research has significantly advanced the understanding of deep cave geochemistry, several aspects require further investigation. Future studies should include more detailed geological mapping at depth, as current geological maps provide only surface-level data and cannot fully explain subsurface variations. Geophysical methods such as seismic profiling could help clarify the distribution of carbonate and non-carbonate rock units. Additionally, stable isotope analysis of heavy metals (e.g., Pb, Sr) could aid in distinguishing between natural and anthropogenic sources. Investigating the role of aeolian dust and past volcanic activity in mineral deposition would also help to better understand the origins of clay minerals and associated elements.

Future research should focus on stable isotope analysis of heavy metals, particularly Pb, to better determine the origin of these anomalies. Further monitoring of atmospheric deposition in the region could also help assess the role of long-range transport of pollutants, as suggested by studies on urban speleothems. Additionally, expanding the spatial and depth range of sampling will improve our understanding of metal transport mechanisms and their implications for karst hydrology and groundwater protection.

**Supplementary Materials:** The following supporting information can be downloaded at the website of this paper posted on Preprints.org, Figure S1; Figure S2; Table S1-S13.

**Author Contributions:** Conceptualization, D.P., S.F.-B. and N.B.; methodology, K.M. and S.F.-B., D.P. and N.B.; software, S.F.-B., D.P.; analysis, S.F.-B., N.B., D.P. and K.M.; investigation, D.P., S.F.-B. and N.B.; collection data in the field, D.P.; writing—original draft preparation, D.P., S.F.-B. and N.B.; writing—review and editing, supervised the work, D.P., S.F.-B. and N.B. All authors have read and agreed to the published version of the manuscript.

**Funding:** This research was partially supported by the Northern Velebit National Park, Croatia and research funding in the Department of Geography at the Faculty of Science, University of Zagreb.

**Data Availability Statement:** The data will be made available on request.

**Acknowledgments:** The authors thank Prof. Nenad Tomašić for assistance with mineralogical analysis. We acknowledge the support provided by the Josip Juraj Strossmayer Water Institute, Main Water Laboratory (MWL), especially Mag. Simana Milović. We thank the members of the Speleological Society Velebit and Speleological Committee of CMA, Zagreb, for their assistance in field work. We also appreciate the journal’s reviewers for taking their precious time to review the manuscript.

**Conflicts of Interest:** The authors declare no conflicts of interest.

Appendix A

**Table A1.** Mineral (phase) composition of speleothem samples. Sign “+” means that sample contains this mineral.

Sample	Calcite	Quartz	Kaolinite	Muscovite	Chlorite	Montmorill.	Magnetite	Goethite	Plagioclase	Dolomite
ZSDV-100	+	+								
ZSDV-101	+									
ZSDV-102	+	+								
ZSDV-103	+	+								
ZSDV-104	+	+	+							
ZSDV-105	+	+		+	+	+				
ZSDV-106	+	+								
ZSDV-107	+	+	+	+	+	+	+			
ZSDV-108	+	+								
ZSDV-109	+	+								
ZSDV-110	+	+		+	+	+	+	+		
ZSDV-111	+									
ZSDV-112	+	+		+	+	+				+
ZSDV-113	+									
ZSDV-114	+	+		+			+			

ZSDV-115	+	+	+	+		+	
ZSDV-116	+	+		+	+		
ZSDV-118	+	+					+
ZSDV-119	+	+	+	+		+	
ZSDV-120	+	+					
ZSDV-121	+	+		+	+		
ZSDV-122	+	+				+	+
ZSDV-123	+						+
ZSDV-124	+	+		+	+		
ZSDV-125	+	+					
ZSDV-126	+	+			+		+
ZSDV-127	+	+	+		+	+	
ZSDV-128	+	+	+	+	+	+	
ZSDV-129	+	+					
ZSDV-130	+	+		+	+	+	+
ZSDV-131	+	+					
ZSDV-132	+						
ZSDV-133	+	+		+	+		+
ZSDV-134	+	+		+	+		
ZSDV-135	+	+	+				
ZSDV-136	+	+					
ZSDV-138	+	+					
ZSDV-139	+	+					
ZSDV-140	+						
ZSDV-141	+						
ZSDV-142	+	+					
ZSDV-143	+	+					
ZSDV-144A	+						

ZSDV-144B	+	+
ZSDV-145	+	

Table A2. Results of ICP-MS analysis of 30 chemical elements in solid samples.

Sample	Al mg/ kg	B mg/ kg	Ba mg/ kg	Be mg/ kg	Bi mg/ kg	Ca mg/ kg	Cd mg/ kg	Co mg/ kg	Cr mg/ kg	Cs mg/ kg	Cu mg/ kg	Fe mg/ kg	K mg/ kg	Li mg/ kg	Mg mg/ kg
ZSDV - 100	473	0,679	6,95	0,033	0,236	81855	0,054	0,391	3,78	0,436	1,62	1618	129	2,66	101
ZSDV - 101	251	0,596	3,20	0,015	0,071	92465	0,040	0,287	4,93	0,532	0,660	558	94,2	5,18	156
ZSDV - 102	472	0,760	8,21	0,036	0,213	74620	0,047	0,470	2,95	0,553	1,20	1387	136	2,75	200
ZSDV - 103	375	0,253	3,60	0,020	0,098	86836	0,044	0,350	3,52	1,0	0,831	793	56,8	2,72	92,6
ZSDV - 104	3502	2,19	35,3	0,156	1,36	49249	0,076	1,29	10,9	6,79	5,76	9876	731	14,1	377
ZSDV - 105	4113	9,96	61,5	0,175	0,664	90203	0,153	1,98	12,4	2,07	4,20	5570	1143	5,56	507
ZSDV - 106	409	1,73	4,85	0,015	0,103	128213	0,043	0,587	3,80	0,252	0,590	517	269	3,77	300
ZSDV - 107	13737	13,1	112	0,452	2,0	3732	0,374	5,64	31,9	4,56	9,30	26293	1923	22,2	738
ZSDV - 108	320	0,363	5,63	0,012	0,053	114421	0,031	0,531	3,58	0,170	0,545	500	76,7	0,618	45,2
ZSDV - 109	180	0,145	7,82	0,016	0,072	87355	0,086	0,450	2,68	0,140	0,750	664	27,5	0,844	105
ZSDV - 110	6171	4,90	71,2	0,273	1,12	26950	0,443	3,44	20,2	3,32	4,62	16480	853	23,9	321
ZSDV - 111	30,8	0,145	0,845	<0,005	0,023	106600	0,017	0,293	2,34	<0,030	0,373	65,6	12,8	0,085	520
ZSDV - 112	1719	0,694	46,4	0,091	0,481	64409	0,069	1,09	6,55	1,12	2,15	4898	569	3,06	389
ZSDV - 113	122	0,144	2,12	0,010	0,044	88824	0,045	0,408	2,41	0,107	0,539	424	22,6	0,619	209
ZSDV - 114	1962	0,602	10,5	0,105	0,323	75638	0,384	1,28	7,38	1,47	2,0	8520	328	9,94	190
ZSDV - 115	1983	0,667	11,4	0,090	0,364	40678	0,232	0,959	7,61	1,19	2,12	6664	327	5,01	125
ZSDV - 116	3938	3,40	40,7	0,195	2,95	35985	0,394	1,62	39,9	4,13	6,92	14301	762	18,1	534
ZSDV - 118	125	0,203	2,71	0,011	0,045	82359	0,018	0,323	1,73	0,168	0,496	361,	42,2	1,11	274
ZSDV - 119	2779	1,26	15,5	0,175	1,18	55298	0,366	2,23	25,6	2,58	4,03	12326	317	14,8	213
ZSDV - 120	19,5	<0,100	13,1	<0,005	<0,030	79182	0,067	0,319	11,6	<0,030	0,441	84,2	8,28	0,047	634
ZSDV - 121	1851	0,804	31,8	0,105	0,884	72333	0,147	1,15	6,50	1,69	2,10	4454	323	3,89	712
ZSDV - 122	923	2,0	7,47	0,035	0,169	66825	0,090	0,600	6,28	0,815	2,23	3845	767	1,09	396
ZSDV - 123	105	0,205	1,57	0,011	0,044	69173	0,020	0,309	2,70	0,064	0,462	459	63,5	0,100	6630
ZSDV - 124	2396	2,13	21,0	0,138	0,715	54126	0,505	1,37	8,49	1,25	3,58	8733	701	4,70	329
ZSDV - 125	11,3	<0,100	0,545	<0,005	0,154	113734	0,072	0,264	12,0	<0,030	0,298	77,5	4,67	0,068	10,3
ZSDV - 126	1505	0,660	23,3	0,078	0,505	71445	0,058	1,02	6,31	1,05	3,67	4241	461	3,23	379
ZSDV - 127	11202	7,18	76,1	0,503	2,46	15950	0,323	5,84	35,8	6,55	7,68	28640	1167	41,8	500



ZSDV - 128	7388	3,74	63,5	0,370	1,71	28058	0,213	3,69	17,8	5,56	6,65	20436	1338	29,5	504
ZSDV - 129	85,9	<0,100	0,917	<0,005	<0,030	94922	0,047	0,319	2,52	0,069	0,460	257	14,6	0,300	19,4
ZSDV - 130	4733	2,05	138	0,302	1,56	13320	0,105	2,62	14,8	3,46	5,98	17600	1502	15,2	1069
ZSDV - 131	12,0	8,35	40,5	12,5	5,40	4,12	0,198	54,2	1,86	72,8	68,2	0,089	0,685	183	4,44
ZSDV - 132	3,70	17,7	9,68	25,6	0,779	2,45	0,495	32,7	1,03	191	32,6	0,047	0,604	123	1,24
ZSDV - 133	12,5	4,52	22,1	6,33	3,04	4,14	0,272	57,5	1,36	125	80,3	0,115	1,03	100	3,41
ZSDV - 134	5,66	5,55	14,5	9,71	1,40	2,16	0,318	44,2	1,19	84,8	49,6	0,061	0,501	114	1,53
ZSDV - 135	47,6	7,07	26,5	16,2	13,0	24,9	0,503	148	1,79	52,0	386	0,700	2,23	147	9,66
ZSDV - 136	115	2,80	132	6,10	7,85	13,0	0,186	108	1,50	26,8	342	0,622	0,912	77,3	9,14
ZSDV - 138	7,91	3,40	82,1	7,44	1,05	1,40	0,081	22,2	0,870	107	36,8	0,075	1,06	81,5	1,07
ZSDV - 139	560	7,67	116	21,7	31,9	43,7	0,782	98,5	2,45	30,7	1068	1,62	4,29	212	24,5
ZSDV - 140	11,0	3,98	16,0	6,85	0,730	1,64	0,250	20,4	0,523	11,3	38,3	0,079	0,292	69,6	0,892
ZSDV - 141	73,3	5,07	11,7	6,83	1,43	0,898	0,150	18,7	1,19	47,0	40,2	0,131	0,600	113	1,27
ZSDV - 142	477	8,24	36,0	18,0	20,2	22,9	0,656	80,7	1,63	38,7	496	1,18	2,25	98,1	14,0
ZSDV - 143	0,767	5,0	29,6	7,35	0,251	0,176	0,359	2,76	1,35	116	5,41	0,009	0,975	137	0,711
ZSDV - 144A	70,6	3,58	31,0	6,14	5,50	11,6	0,098	76,5	0,830	85,5	287	0,264	0,900	68,4	4,10
ZSDV - 144B	16,1	5,08	15,2	7,20	0,827	0,650	0,039	15,0	1,22	93,4	29,0	0,038	0,870	104	0,739
ZSDV - 145	126	5,45	17,3	7,50	6,76	7,66	0,202	106	0,772	18,1	214	0,308	0,920	76,7	5,08

Table A3. Results of ICP-MS analysis of 30 chemical elements in three water samples.

Sample	Al µg/L	As µg/L	B µg/L	Ba µg/L	Be µg/L	Ca mg/L	Cd µg/L	Co µg/L	Cr µg/L	Cs µg/L	Cu µg/L	Fe µg/L	K mg/L	Li µg/L	Mg mg/L
M07	30,3	0,441	2,85	5,45	<0,005	37,1	0,020	0,097	0,260	<0,030	1,72	38,4	0,900	0,226	<0,500
M10	19,7	0,380	2,49	3,93	<0,005	34,8	<0,010	0,085	0,127	<0,030	2,33	13,7	0,200	0,227	<0,500
M20	64,1	0,355	2,85	3,70	<0,005	35,1	<0,010	0,090	0,162	<0,030	1,06	14,3	0,250	0,157	<0,500
Sample	Mn µg/L	Mo µg/L	Na mg/L	Ni µg/L	Pb µg/L	Rb µg/L	Sb µg/L	Si mg/L	Sn µg/L	Sr µg/L	Ti µg/L	Tl µg/L	U µg/L	V µg/L	Zn µg/L
M07	1,22	0,088	0,860	0,557	0,411	0,475	0,207	1,30	0,060	29,0	0,732	0,004	0,212	0,443	1,58
M10	0,509	0,043	0,620	2,90	0,190	0,216	0,036	1,16	<0,020	30,1	0,579	<0,003	0,153	0,316	1,38
M20	0,607	0,065	0,610	0,649	<0,010	0,237	0,081	1,04	<0,020	27,8	0,534	<0,003	0,141	0,283	1,28

Table A4. Anomalies (extremes and outliers) determined by boxplot method.

Sample	Extreme	Outlier
ZSDV -100	-	-
ZSDV -101	-	Sr
ZSDV -102	-	-
ZSDV -103	-	-
ZSDV -104	-	Cs
ZSDV -105	B, Na	-
ZSDV -106		Na
ZSDV -107	Al, B, Co, Mn, Na, Tl	Ba, Be, Cr, Cu, Fe, K, Pb, Rb, Ti, U, Zn

ZSDV -108	-	-
ZSDV -109	-	-
ZSDV -110	Mn	Co, Tl
ZSDV -111	-	-
ZSDV -112	-	-
ZSDV -113	-	-
ZSDV -114	-	-
ZSDV -115	-	-
ZSDV -116	Mo, Ni, Pb	Bi, Cr
ZSDV -118	-	Sb
ZSDV -119	Mo, Ni	-
ZSDV -120	Mo, Sr	Ni
ZSDV -121	Sr	-
ZSDV -122	-	-
ZSDV -123	Mg	-
ZSDV -124		Cd
ZSDV -125	Mo, Ni	-
ZSDV -126	-	-
ZSDV -127	Al, Co, Li, Tl	B, Be, Bi, Cr, Cs, Fe, Pb, Rb, Zn
ZSDV -128	-	Al, Co, Li, Mn, Na, Pb, Tl
ZSDV -129	-	-
ZSDV -130	Ba, Na	Rb
ZSDV -131	Cd, Cr, Mo, Ni	-
ZSDV -132	Mo	Cr, Ni
ZSDV -133	-	Ba, Be, Na
ZSDV -134	-	-
ZSDV -135	-	-
ZSDV -136	-	-
ZSDV -138	-	-
ZSDV -139	-	-
ZSDV -140	Mo, Ni	Cr
ZSDV -141	-	-
ZSDV -142	Cs, Mo, Ni	-
ZSDV -143	-	-
ZSDV -144A	-	-
ZSDV -144B	Cr, Mo, Ni	Cd
ZSDV -145	Na	-

Table A5. Members of obtained clusters and distances from respective cluster centers.

Cluster Number 1		Cluster Number 2		Cluster Number 3	
	Distance		Distance		Distance
ZSDV-100	2296,907	ZSDV-101	986,315	ZSDV-107	3840,709
ZSDV-102	1160,563	ZSDV-103	1949,649	ZSDV-110	707,108
ZSDV-104	3505,504	ZSDV-105	1746,685	ZSDV-115	3650,59
ZSDV-112	780,491	ZSDV-106	5148,341	ZSDV-116	2335,307
ZSDV-114	1327,349	ZSDV-108	2782,85	ZSDV-127	2383,742
ZSDV-118	2442,552	ZSDV-109	1859,763	ZSDV-128	995,872
ZSDV-119	2682,862	ZSDV-111	1447,447	ZSDV-130	1696,761
ZSDV-120	2068,802	ZSDV-113	1608,54	ZSDV-133	630,79

<b>ZSDV-121</b>	615,082	<b>ZSDV-125</b>	2667,503	<b>ZSDV-134</b>	857,839
<b>ZSDV-122</b>	428,126	<b>ZSDV-129</b>	568,616		
<b>ZSDV-123</b>	1283,476	<b>ZSDV-131</b>	1669,34		
<b>ZSDV-124</b>	2634,997	<b>ZSDV-132</b>	1892,675		
<b>ZSDV-126</b>	454,429	<b>ZSDV-138</b>	241,428		
<b>ZSDV-135</b>	3506,321	<b>ZSDV-139</b>	113,224		
<b>ZSDV-136</b>	979,731	<b>ZSDV-140</b>	851,933		
<b>ZSDV-141</b>	2363,343	<b>ZSDV-142</b>	923,613		
		<b>ZSDV-143</b>	1501,29		
		<b>ZSDV-144A</b>	1315,248		
		<b>ZSDV-144B</b>	1271,849		
		<b>ZSDV-145</b>	274,117		

**Table A6.** Mean values of 10 elements and two other parameters for 3 obtained clusters. Element's contents are given in mg/kg, elevation in m.

	<b>Cluster - No. 1</b>	<b>Cluster - No. 2</b>	<b>Cluster - No. 3</b>
<b>Cave</b>	<b>1,19</b>	<b>1,50</b>	<b>1,33</b>
<b>Depth</b>	<b>664,25</b>	<b>440,25</b>	<b>323,89</b>
<b>Al</b>	<b>1402,22</b>	<b>352,46</b>	<b>6420,78</b>
<b>B</b>	<b>1,04</b>	<b>0,86</b>	<b>4,40</b>
<b>Ba</b>	<b>17,68</b>	<b>5,55</b>	<b>79,56</b>
<b>Be</b>	<b>0,08</b>	<b>0,02</b>	<b>0,32</b>
<b>Bi</b>	<b>0,48</b>	<b>0,10</b>	<b>1,72</b>
<b>Ca</b>	<b>68916,31</b>	<b>98196,25</b>	<b>23043,11</b>
<b>Cd</b>	<b>0,13</b>	<b>0,13</b>	<b>0,26</b>
<b>Co</b>	<b>0,91</b>	<b>0,46</b>	<b>3,06</b>
<b>Cr</b>	<b>7,50</b>	<b>23,33</b>	<b>30,18</b>
<b>Cs</b>	<b>1,47</b>	<b>5,56</b>	<b>4,00</b>
<b>Cu</b>	<b>2,24</b>	<b>0,75</b>	<b>5,82</b>
<b>Fe</b>	<b>4795,51</b>	<b>644,85</b>	<b>17686,45</b>
<b>K</b>	<b>353,35</b>	<b>101,23</b>	<b>1105,11</b>
<b>Li</b>	<b>4,90</b>	<b>1,24</b>	<b>20,72</b>
<b>Mg</b>	<b>725,63</b>	<b>153,69</b>	<b>608,00</b>
<b>Mn</b>	<b>53,62</b>	<b>13,11</b>	<b>248,00</b>
<b>Mo</b>	<b>12,66</b>	<b>66,92</b>	<b>19,33</b>
<b>Na</b>	<b>19,88</b>	<b>33,59</b>	<b>71,88</b>
<b>Ni</b>	<b>19,66</b>	<b>100,34</b>	<b>35,48</b>
<b>Pb</b>	<b>5,99</b>	<b>1,02</b>	<b>27,53</b>
<b>Rb</b>	<b>9,40</b>	<b>1,45</b>	<b>31,43</b>
<b>Sb</b>	<b>0,36</b>	<b>0,22</b>	<b>0,49</b>
<b>Si</b>	<b>86,01</b>	<b>20,21</b>	<b>113,50</b>
<b>Sn</b>	<b>1,21</b>	<b>1,10</b>	<b>2,00</b>

Sr	405,19	63,50	46,96
Ti	204,47	39,59	599,00
Tl	0,26	0,07	0,96
U	1,46	0,68	2,39
V	106,01	128,59	123,47
Zn	4,55	1,40	16,02

Table A7. Factor Loadings (varimax normalized; Marked loadings are &gt;0.7).

	Factor - 1	Factor - 2	Factor - 3
Depth	-0,124302	-0,023993	<b>-0,819019</b>
Al	<b>0,954821</b>	0,040576	0,065068
Be	<b>0,964641</b>	0,013376	0,052559
Ca	<b>-0,910654</b>	-0,035486	0,071048
Cd	0,367832	<b>0,870409</b>	0,002824
Co	<b>0,943561</b>	0,088319	0,060373
Cr	0,097057	<b>0,956666</b>	0,030635
Cu	<b>0,965842</b>	0,043518	0,106860
Fe	<b>0,987710</b>	0,045008	0,063385
Li	<b>0,928842</b>	0,059540	0,121091
Mn	<b>0,860786</b>	0,107496	0,059534
Ni	-0,183442	<b>0,940852</b>	0,034932
Pb	<b>0,792268</b>	0,117471	0,138042
Si	<b>0,722576</b>	0,023701	0,062805
Sr	-0,060724	-0,024627	<b>-0,804648</b>
Zn	<b>0,979650</b>	0,057248	0,111071
Expl.Var	9,380962	2,606750	1,405087
Prp.Totl	0,586310	0,162922	0,087818

Table A8. Factor Scores for analyzed samples.

	Factor - 1	Factor - 2	Factor - 3
ZSDV-100	-0,44969	-0,468335	0,91344
ZSDV-101	-0,66168	-0,423453	0,83505
ZSDV-102	-0,44930	-0,507157	0,74082
ZSDV-103	-0,61171	-0,481194	0,81870
ZSDV-104	0,65183	-0,469277	0,74884
ZSDV-105	0,34543	-0,280647	0,72149
ZSDV-106	-0,77655	-0,455562	0,83723
ZSDV-107	2,91683	0,220452	0,07686
ZSDV-108	-0,76396	-0,477140	0,54742



<b>ZSDV-109</b>	-0,59976	-0,389911	0,39858
<b>ZDSV-110</b>	1,57251	1,230746	0,06671
<b>ZDSV-111</b>	-0,80161	-0,501358	0,12572
<b>ZSDV-112</b>	-0,03876	-0,442072	-0,02598
<b>ZSDV-113</b>	-0,68940	-0,468341	0,36007
<b>ZSDV-114</b>	0,18179	0,138592	0,29450
<b>ZSDV-115</b>	0,16931	-0,151257	0,20318
<b>ZSDV-116</b>	1,48445	0,983193	0,95783
<b>ZSDV-118</b>	-0,70573	-0,550535	0,84204
<b>ZSDV-119</b>	0,88586	0,531137	0,26291
<b>ZSDV-120</b>	-0,34931	-0,095727	-4,94046
<b>ZSDV-121</b>	0,13086	-0,249879	-2,03191
<b>ZSDV-122</b>	-0,13940	-0,339670	-1,09632
<b>ZSDV-123</b>	-0,56206	-0,484421	-1,03985
<b>ZSDV-124</b>	0,47950	0,399545	-1,17644
<b>ZSDV-125</b>	-0,87972	-0,012148	0,13909
<b>ZSDV-126</b>	-0,01168	-0,483615	0,24995
<b>ZSDV-127</b>	2,75371	0,126628	0,10225
<b>ZSDV-128</b>	1,96719	-0,195167	0,15930
<b>ZSDV-129</b>	-0,76242	-0,443131	0,47835
<b>ZSDV-130</b>	1,28806	-0,439484	0,58186
<b>ZSDV-131</b>	-0,82480	4,817560	-0,06662
<b>ZSDV-132</b>	-0,72776	0,154602	0,02479
<b>ZSDV-133</b>	1,22900	-0,462031	-0,21315
<b>ZSDV-134</b>	1,10399	-0,353444	-0,18035
<b>ZSDV-135</b>	0,67268	-0,338948	-0,41738
<b>ZSDV-136</b>	-0,08725	-0,449788	-0,31604
<b>ZSDV-138</b>	-0,71929	-0,485320	-0,28463
<b>ZSDV-139</b>	-0,70896	-0,517329	-0,27965
<b>ZSDV-140</b>	-0,74195	1,245226	-0,42709
<b>ZSDV-141</b>	-0,59604	-0,507463	-0,55998
<b>ZSDV-142</b>	-0,72349	0,332592	-0,55415
<b>ZSDV-143</b>	-0,86040	-0,486455	0,96571
<b>ZSDV-144A</b>	-0,85409	-0,514546	0,99775
<b>ZSDV-144B</b>	-1,02319	3,184189	0,74276
<b>ZSDV-145</b>	-0,71303	-0,439658	-0,58319

Table A9. Magnetic susceptibility measured in cave samples from Velebit Mt.

Sample	ZSDV - 100	ZSDV - 101	ZSDV - 102	ZSDV - 103	ZSDV - 104	ZSDV - 105	ZSDV - 106	ZSDV - 107	ZSDV - 108	ZSDV - 109	ZSDV - 110
MS (10 <sup>-3</sup> SI units)	0.008	0.000	0.014	0.000	0.047	0.043	0.002	0.168	0.002	0.001	0.064
Sample	ZSDV - 111	ZSDV - 112	ZSDV - 113	ZSDV - 114	ZSDV - 115	ZSDV - 116	ZSDV - 118	ZSDV - 119	ZSDV - 120	ZSDV - 121	ZSDV - 122
MS (10 <sup>-3</sup> SI units)	0.000	0.094	0.000	0.026	0.009	0.070	0.000	0.038	0.000	0.033	0.005
Sample	ZSDV - 124	ZSDV - 125	ZSDV - 126	ZSDV - 127	ZSDV - 128	ZSDV - 129	ZSDV - 130	ZSDV - 131	ZSDV - 132	ZSDV - 133	ZSDV - 134
MS (10 <sup>-3</sup> SI units)	0.015	0.001	0.099	0.024	0.069	0.002	0.152	0.003	0.002	0.089	0.060
Sample	ZSDV - 135	ZSDV - 136	ZSDV - 138	ZSDV - 139	ZSDV - 140	ZSDV - 141	ZSDV - 142	ZSDV - 143	ZSDV - 144A	ZSDV - 144B	ZSDV - 145
MS (10 <sup>-3</sup> SI units)	0.042	0.008	0.002	0.005	0.001	0.000	0.003	0.000	0.002*	0.001*	0.000

Table A10. Correlations between MS and determined chemical elements. Correlations are significant at p < ,05000 N=45.

	Al	B	Ba	Be	Bi	Ca	Cd	Co	Cr	Cs	Cu	Fe	K	Li	Mg
MS	0,73	0,59	0,87	0,75	0,71	-0,75	0,19	0,69	0	-0,01	0,8	0,74	0,84	0,57	0,09
	Mn	Mo	Na	Ni	Pb	Rb	Sb	Si	Sn	Sr	Ti	Tl	U	V	Zn
MS	0,7	-0,15	0,56	-0,14	0,6	0,81	0,31	0,59	0,53	-0,1	0,78	0,64	0,51	0,04	0,72

References

1. Bognar, A.; Faivre, S.; Buzjak, N.; Pahernik, M.; Bočić, N. Recent Landform Evolution in the Dinaric and Pannonian Regions of Croatia. In *Recent Landform Evolution: The Carpatho–Balkan–Dinaric Region*; Lóczy, D., Stankoviansky, M., Kotarba, A., Eds.; Springer: Cham, Switzerland, 2012; pp. 313–344.

2. White, W. B. *Cave Geology*; Cambridge University Press: Cambridge, UK, 2007.

3. Sasowsky, I.D.; Mylroie, J. *Studies of Cave Sediments: Physical and Chemical Records of Paleoclimate*; Springer: Dordrecht, The Netherlands, 2004.

4. Paar, D.; Frančičković-Bilinski, S.; Buzjak, N.; Maldini, K.; Milović, S.; Pichler, S. Geochemical and Mineralogical Characterization of Speleothems from the Karst of Croatia as Potential Sources of Data for Environmental Research. *J. Geochem. Explor.* 2016, 167, 20–37.

5. Surić, M. Speleothem-Based Quaternary Research in Croatian Karst – A Review. *Quat. Int.* 2018, 490, 113–122.

6. Höpker, R.; Müller, T.; Schmidt, F.; Becker, J. Recent Developments in Cave Sediment Studies. *J. Karst Res.* 2024, 58, 233–245.

7. Çil, E.; Kaya, Ö.; Yılmaz, H.; Demir, A. Speleothem Geochemistry and Paleoenvironmental Interpretations. *Earth Sci. J.* 2023, 49, 120–135.

8. Muri, G.; Kralj, P.; Krajcar Bronić, I.; Horvatinčić, N. Karst Aquifers and Their Vulnerability to Contamination. *Hydrogeol. J.* 2013, 21, 765–779.

9. Chen, J.; Wang, S.; Liu, Y.; Zhang, Q.; Zhao, H. Groundwater Extraction from Karst Aquifers: A Global Perspective. *Water Resour. Res.* 2017, 53, 890–905.

10. Kuhta, M.; Brkić, M. Hydrogeochemical Dynamics of Karst Systems. *Environ. Geol.* 2008, 56, 567–580.

11. Paar, D.; Mance, D.; Stroj, A.; Pavić, M. Northern Velebit (Croatia) Karst Hydrological System: Results of a Preliminary <sup>2</sup>H and <sup>18</sup>O Stable Isotope Study. *Geol. Croat.* 2019, 72, 205–213.

12. Addesso, R.; De Waele, J.; Cafaro, S.; Baldantoni, D. Geochemical Characterization of Clastic Sediments Sheds Light on Energy Sources and on Alleged Anthropogenic Impacts in Cave Ecosystems. *Int. J. Earth Sci.* 2022, 111, 919–927.

13. Rozkowski, J.; Rozkowski, K.; Rahmonov, O. Heavy Metals in the Unsaturated and Saturated Zone of the Upper Jurassic Carbonate Massif in the Vicinity of Krakow. *J. Elementol.* 2015, 20, 395–406.

14. Pons-Branchu, E.; Takahashi, C.; Frisia, S.; Borsato, A. Urban Speleothems as Records of Heavy Metal Pollution. *Sci. Total Environ.* 2015, 512, 435–448.
15. Allan, M.; Fagel, N.; Van Rampelbergh, M.; Baldini, J.; Riotte, J.; Cheng, H.; Edwards, R.L.; Gillikin, D.; Quinif, Y.; Verheyden, S. Lead Concentrations and Isotope Ratios in Speleothems as Proxies for Atmospheric Metal Pollution Since the Industrial Revolution. *Chem. Geol.* 2015, 401, 140–150.
16. Xu, H.; Li, Y.; Wang, X.; Zhang, L. Heavy Metal Contamination in Cave Water Systems. *Hydrogeol. Contam. Transp.* 2020, 12, 123–135.
17. Zeng, J.; Han, G.L.; Yang, K.H. Assessment and Sources of Heavy Metals in Suspended Particulate Matter in a Tropical Catchment, Northeast Thailand. *J. Clean. Prod.* 2020, 265, Article 121898.
18. Zupan Hajna, N. Speleothem Records and Karst Hydrology. *J. Karst Hydrogeol.* 2011, 28, 403–415.
19. Surić, D.; Barešić, J.; Lončar, T.; Peh, Z. Evolution of Speleothem Deposition in Croatian Caves: Implications for Paleoenvironmental Changes. *J. Karst Geochem.* 2005, 21, 105–120.
20. Surić, D.; Perica, D.; Tibljaš, D. Multi-Year Geochemical Analysis of Speleothems: A New Perspective on Karst Hydrology. *Geochim. Cosmochim. Acta* 2009, 73, 245–260.
21. Bonacci, O. *Karst Hydrology: With Special Reference to Dinaric Karst*; Springer-Verlag: Berlin, Germany, 1987.
22. Boldrin, A.; Juračić, M.; Mengazzo Vitturi, L.; Rabitti, S.; Rampazzo, G. Sedimentation of River-Borne Material in a Shallow Shelf Sea: Adiga River, Adriatic Sea. *Mar. Geol.* 1992, 103, 473–485.
23. StatSoft, Inc. *STATISTICA (Data Analysis Software System), Version 6*; StatSoft, Inc.: 2001. Available online: [www.statsoft.com](http://www.statsoft.com).
24. Tukey, J.W. *Exploratory Data Analysis*; Addison-Wesley: Reading, PA, USA, 1977.
25. Reimann, C.; Filzmoser, P.; Garrett, R.G. Background and Threshold: Critical Comparison of Methods of Determination. *Sci. Total Environ.* 2005, 346, 1–16.
26. Kaufman, L.; Rousseeuw, P. *Finding Groups in Data*; John Wiley & Sons: New York, NY, USA, 1990.
27. Halamić, J.; Peh, Z.; Bukovec, D.; Miko, S.; Galović, L. A Factor Model of the Relationship Between Stream Sediment Geochemistry and Adjacent Drainage Basin Lithology, Medvednica Mt., Croatia. *Geol. Croat.* 2001, 54, 37–51.
28. Davis, J.C. *Statistics and Data Analysis in Geology*, 3rd ed.; John Wiley & Sons: Hoboken, NJ, USA, 2002.
29. Frančisković-Bilinski, S.; Scholger, R.; Bilinski, H.; Tibljaš, D. Magnetic, Geochemical and Mineralogical Properties of Sediments from Karst and Flysch Rivers of Croatia and Slovenia. *Environ. Earth Sci.* 2014, 72, 3939–3953.
30. Pons-Branchu, E.; Ayrault, S.; Roy-Barman, M.; Bordier, L.; Borst, W.; Branchu, P.; Douville, E.; Dumont, E. Three Centuries of Heavy Metal Pollution in Paris (France) Recorded by Urban Speleothems. *Sci. Total Environ.* 2015, 518, 86–96.

**Disclaimer/Publisher's Note:** The statements, opinions and data contained in all publications are solely those of the individual author(s) and contributor(s) and not of MDPI and/or the editor(s). MDPI and/or the editor(s) disclaim responsibility for any injury to people or property resulting from any ideas, methods, instructions or products referred to in the content.